Journal of Ginseng Research 48 (2024) 543–551

Contents lists available at ScienceDirect

Journal of Ginseng Research

journal homepage: www.sciencedirect.com/journal/journal-of-ginseng-research

Research Article

Investigation of the whitening activity of ginsenosides from Panax notoginseng and optimization of the dosage form

Zeyu Wang [a,1], Daiyan Zhang [a,1], Mingju Shui [a,1], Ian Wa Ho [b,c], Weng Si Kou [b,c], Jianwen Wei [a,c], Jian-Bo Wan [a], Ruibing Wang [a,*], Qing-Wen Zhang [a,*]

[a] State Key Laboratory of Quality Research in Chinese Medicine, Institute of Chinese Medical Sciences, University of Macau, Macao SAR, China
[b] Pui Chng Middle School (Macau), Macao SAR, China
[c] Macau Society of Supramolecular Chemistry and Biomaterials, Macao SAR, China

ARTICLE INFO

Keywords:
Panax notoginseng
Ginsenoside
Ethosome
Transdermal delivery
Natural product whitening

ABSTRACT

Background: Ginsenoside, as an active ingredient in traditional Chinese medicine, has been widely used for skin whitening for several years. Recent research has found that Panax notoginseng has a higher content of ginsenosides compared with the Panax ginseng. Those ginsenosides have promising potential to be developed as skin whitening agents.

Methods: We selected five dammarane ginsenosides isolated from P. notoginseng and their mixtures to investigate the skin lightning activity. Zebrafish embryo model was used for initial screening of the whitening activity. Subsequently, the whitening effect of components was examined and compared via testing the inhibition of melanin and activity of tyrosinase in B16 cells treated with these components. Molecular docking was also applied to investigate the interactions between ginsenosides and tyrosinase. Finally, the most effective saponins were selected for dosage form optimization and the whitening effect of saponin-loaded ethosomes was further demonstrated on the C57BL/6 mouse model.

Results: Experimental results showed that the protopanaxtriol saponins (PTS) were the most potent saponins with a decent safety profile, and the molecule docking results demonstrated that PTS had strong inhibitory ability to tyrosinase. PTS was successfully encapsulated into ethosomes with an encapsulation efficiency of 93%. The PTS ethosome gel could effectively inhibit the melanin production caused by UVB tanning on the back skin of mice.

Conclusion: The PTS ethosome gel provides an effective and safe formulation of PTS to whiten the UVB-tanned skin in vivo and could be used as a potential skin whitening agent in the future.

1. Introduction

Ginsenosides, as a natural component with high safety, has been well known for its skin whitening effects for hundreds of years, and has been frequently used in cosmetic products for skin-whitening [1]. However, the high cost of ginseng itself, the low ginsenoside content in ginseng and the difficulty of synthesizing ginsenosides are still the main reasons that prevent the industrialization of whitening products containing ginsenosides [2–4]. Meanwhile, with a lower cost due to mass production, P. notoginseng also contains a variety of dammarane-type ginsenosides, mainly PTS and protopanaxdiol saponins (PDS) [5,6]. In our previous work, we found that three PTS (ginsenosides Rg1 and Re, and notoginsenside R1) and two PDS (ginsenosides Rb1 and Rd) were the major ginsenosides in P. notoginseng [7–10]. Herein, we employed the five major ginsenosides and their mixtures (PTSs and PDSs) from P. notoginseng to further evaluate their whitening effects.

However, due to the high hydrophilicity of ginsenosides, they barely cross the skin barrier, which limits their skin-whitening effects [9]. The melanin production can be restricted in several steps, including by inhibition of gene expression related to tyrosinase and direct activity

* Corresponding authors. State Key Laboratory of Quality Research in Chinese Medicine, Institute of Chinese Medical Sciences, University of Macau, Macao SAR, 999078, China.

E-mail addresses: yc17522@um.edu.mo (Z. Wang), yc07528@um.edu.mo (D. Zhang), mb95808@um.edu.mo (M. Shui), 1002684-3@g.puiching.edu.mo (I.W. Ho), wengsi0311@gmail.com (W.S. Kou), jianwenwei@um.edu.mo (J. Wei), jbwan@um.edu.mo (J.-B. Wan), rwang@um.edu.mo (R. Wang), qwzhang@um.edu.mo (Q.-W. Zhang).

[1] These authors contributed equally to this work.

https://doi.org/10.1016/j.jgr.2023.12.005
Received 16 December 2022; Received in revised form 14 December 2023; Accepted 27 December 2023
Available online 7 January 2024

inhibition of the related enzyme during the synthesis of melanin [11]. The production of melanin takes place in melanocytes which are special cells located at the bottom of the skin epidermis [12]. Thus, the ginsenosides absorption efficiency into skin needs to be improved for achieving better whitening effects in the skin in vivo.

As a new transdermal drug delivery carrier, ethosome, which is optimized from traditional liposomes, a new type of liposome with high deformability, and encapsulation rate, can efficiently penetrate through the skin [13,14]. It has the properties of ordinary liposomes that are mainly composed of amphiphilic molecules, leading to facile self-assembly into bilayer vesicular structures. The higher ethanol content in the ethosome disrupts the orderly distribution of the phospholipid bilayer and increases its lipid mobility, while the increased flexibility of the entire ethosome system due to the presence of ethanol allows the vesicles to pass through the stratum corneum bilayer and ultimately achieve deeper drug delivery [15]. Herein, we selected five main saponins and their separation mixtures in the P. notoginseng for whitening effective assessments on both zebrafish embryo and B16 mouse melanoma cells [16–20]. Subsequently, the most effective components of ginsenosides from P. notoginseng were selected for optimized formulation into ethosome dosage form. Moreover, the whitening effect of the ethosome formulation was verified in the UVB tanning C57BL/6 mouse model, and the results showed that the ethosome formula successfully improved the skin absorption of PTS ginsenoside, which significantly improved the whitening effect on C57BL/6 mouse when compared with the free ginsenoside [21,22]. The results of molecular docking simulation further suggested that the effect of PTS was via the tyrosinase inhibitory pathway.

2. Materials and methods

2.1. Materials

Ginsenosides Rg1, Re, Rb1 and Rd, notoginsenoside R1, PTS and PDS were separated in our laboratory by the previously reported methods [9,23]. Alpha-Melanocyte-stimulating hormone (α-MSH) was purchased from Sigma-Aldrich (Hong Kong). Dulbecco's Modified Eagle Medium (DMEM) and fetal bovine serum (FBS) were obtained from Gibco (USA). 3-(4,5-dimethyl-2-thiazolyl)-2,5-diphenyl-2-H-tetrazolium bromide (MTT) was supplied by Amresco. RIPA Lysis Buffer was purchased from Beyotime Biotechnology (Shanghai). All other chemical reagents were purchased from Aladdin (China). A Milli-Q Integral system (manufactured by Merck) was used to supply Milli-Q water for our studies. All reagents and solvents were used as supplied without further purification.

2.2. In vitro toxicity

293T and B16 cell lines were purchased from ATCC (USA), where they were authenticated by cell vitality test, isozyme detection, DNA fingerprinting, and mycoplasma detection. The cytotoxicity of ginsenosides against B16 and 293T cells was examined via MTT assays. In brief, B16 cells were seeded in 96-well plates with 8×10^3 cells/well density in 100 μL of fresh culture medium for 24 h. The cells were subsequently incubated with a fresh medium (100 μL) containing various concentrations of different ginsenosides at indicated concentrations for additional 48 h. The cellular viability was analyzed via MTT assays with the assistance of a multi-mode microplate reader (FlexStation 3, USA). The same experiment was performed with 293T cells.

2.3. In vitro whitening evaluation

The determination of melanin followed previous method [24]. B16 cells were seeded in 24-well plates at a density of 2×10^5 cells/mL and cultured in Dulbecco's Modified Eagle's Medium (DMEM) containing 10% (v/v) fetal bovine serum at 37 °C in an atmosphere of 5% (v/v) CO_2 in air for 24 h. After 24 h, different ginsenosides at indicated concentrations were applied firstly for 1 h and then they were exposed to α-MSH (20 nM). After culturing for 48 h, all the cells were harvested and 0.5 mL 1 N NaOH solution was used for cell suspension, maintaining at in the water of 80 °C for 50 min. After that the whole solution was then sonicated for 60 min and the melanin content was determined with absorbance at 405 nm. The protein content of the cell lysates was used for data normalization. We used a BCA protein assay kit (Thermo scientific Inc., USA) for the determination of the protein concentration of cell lysates. The result was expressed as a percentage of the activity of the control group cells in the presence of α-MSH. 1-phenyl 2-thiourea (PTU) (0.15 μM) was used as the control. The tyrosinase activity was determined according to the previously reported method [25]. After 48h exposure to different ginsenosides in the absence or presence of 20 nM α-MSH, B16 cell were washed in PBS for three times and then lysed in cold lysis buffer, accompanied with sustained sonication on ice. Then the entire samples were centrifuged at 13,000 rpm for 30 min at 4 °C (Eppendorf, 5315 D, Hamburg, Germany), and the upper layer was used for determination of protein content by using BCA protein assay kit as the standard. The remaining upper layer was used for the activity test of tyrosinase. By using 1 mL of reaction mixture containing 400 μg of the supernatant protein, 2.5 mM L-DOPA and 50 mM phosphate buffer (pH 6.8). We finally determined the absorbance at 475 nm and the mixture was kept at 37 °C prior to testing. The final activity was expressed as a percentage of the activity of the control group cells in the presence of α-MSH. 1-phenyl 2-thiourea (PTU) (0.15 μM) was used as the positive control.

2.4. Decoloring effect screening and toxicity evaluation using zebrafish embryos

The animal experiment was approved by the Animal Ethics Committee, University of Macau. Wild-type zebrafish were maintained as described in the Zebrafish Handbook. Adult zebrafish were kept in a controlled environment at 28.5 °C, under a 14 h light/10 h dark cycle. They were fed general tropical fish food once daily and live brine shrimp twice daily. The generation of zebrafish embryo were applied by natural pairwise mating. And the collection was finished in screen mesh, and then the fish were raised in the cultivated media in dish, with a stable temperature of 28.5 °C in an incubator. Then live embryos were separated into different groups (8–12 in each group) for hatching. To screen decoloring agents, 10 hpf (hour post fertilization) embryos were incubated in a 24-well plate, with 10 embryos per well, containing 1 mL of embryo medium. All the ginsenosides were dissolved in embryo medium, applied to each well, and decoloring evaluations were performed at 48 hpf. 1-phenyl 2-thiourea (PTU) (0.15 mM) was used as the positive control. The toxicity of different ginsenosides towards zebrafish embryos was also assessed. To acquire images, embryos were anesthetized in tricaine, and mounted in 3% methylcellulose. Images were acquired using an Olympus Spinning Disk Confocal Microscope System (IX81 Motorized Inverted Microscope [w/ZDC], IX2 universal control box, X-cite series 120, DP71 CCD Camera; Olympus, Tokyo, Japan).

2.5. Measurement of the melanin content and activity of tyrosinase in zebrafish embryos

Measurements of the melanin contents and tyrosinase activity were determined according to previously reported methods [26]. After treatment with different ginsenosides for 72 h, 50 zebrafish embryos of 10 hpf in each group were collected and then lysed in RIPA Lysis Buffer solution. The lysate was then applied with centrifugation at 12,000 rpm for 5 min. After centrifugation, the upper phase was collected for tyrosinase activity test. By using a 96-well plate, the same amount of both the upper layer and 1 mM L-3,4-dihydroxyphenylalanine (L-DOPA) were added together for incubation at 37 °C for 1 h. Finally, the results were shown as the absorbance at 475 nm. The pellet was also collected

for the determination of the melanin content. We dissolved different groups of the pellets in 1 mL of 1 N NaOH and kept the mixture in 100 °C water bath for 50 min. After all the pellets were dissolved, we transferred the mixture into a 96-well plate and measured solution absorbance at 405 nm. 1-Phenyl 2-thiourea (PTU) was used as the positive control. The final result was expressed as a percentage of the result to the control group. All experiments were performed for three times.

2.6. Molecular docking study

The homology modeling is usually performed to study substrate's interactions with tyrosinase [27–29]. The PPO3 protein (PDB ID:2Y9X, Resolution: 2.78 Å), a tyrosinase from Agaricus bisporus was chosen as the docking target. The crystal structure of target was downloaded from the RCSB PDB and only X-RAY structures having a resolution less than 3 Å were selected and saved as *pdb* format. The ligand and receptor were split by discovery studio 4.5 [30]. Autodock Tools was used to prepare the *pdbqt* format files. The gird boxes were adjusted to cover the entire pocket. After getting the related files of protein, we searched compounds information from Pubchem database, which were saved as *sdf* format and transformed into *pdbqt* format by Openbabel to dock in the next step. Autodock Vina1.1.2 was used to simulate the potential interactions among the selected compounds and the targets [31,32].

2.7. Preparation and characterization of PTS ethosome

The ethosome formulation was composed of 9% soybean lecithin, 4% cholesterol, 20% ethanol, PTS as described and water to 100% w/w [33]. Briefly, soybean lecithin and cholesterol were dissolved in ethanol. PTS dissolved in Milli-Q water was added slowly drop by drop under sonication. For prevention of the evaporation of ethanol, the entire reaction system maintained airtight. After slowly mixing the two different phages for 10 min, the system was kept in a stable state in sonication bath at 40 °C. Finally, the suspension was finely homogenized. A colloidal solution was obtained through a 0.22 μm disposable filter (Model lf1, Avestin, Canada) to form uniform sized PTS ethosomes.

2.8. Characterization of PTS ethosome

Ethosome vesicles were visualized using a transmission electron microscopy (TEM, JEOL 2100F, Japan) at the operation voltage of 200 kV. Ethosomal solution (10 μL) was dried on a microscopic carbon-coated grid for staining. The excess solution was removed by blotting. Samples were negatively stained with a 1% aqueous solution of PTA before observation. The size distribution and zeta potential of colloidal ethosome were determined via dynamic light scattering (DLS) using a computerized inspection system (Malvern Zetamaster ZEM 5002, Malvern, UK). For size measurements, ethosome suspension was mixed with

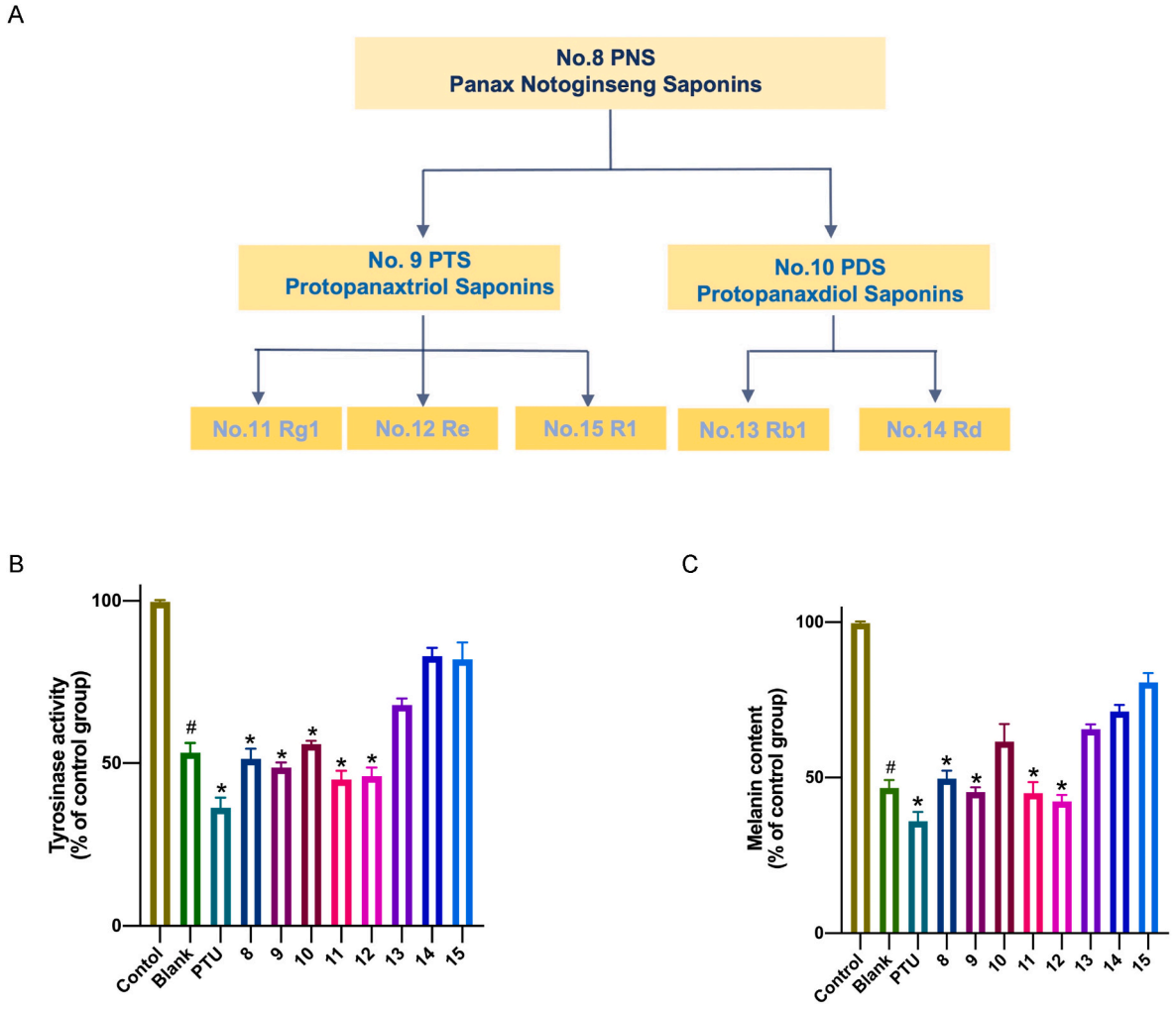

Fig. 1. Relationship and whitening effects of saponions. (A) Relationship between different saponins and the mixtures and (B) Inhibition effects of different ginsenosides at the same concentration of 0.1 mg/mL on B16 cell and (C) The Melanin content of B16 cell after treated with different saponin at the same concentration of 0.1 mg/mL. All the groups were treated with 20 nM α-MSH except the blank group. The data are expressed as a mean value ± SD of three independent experiments. Data analyses were all one-way t-tests for comparisons with the CONTROL group, *P ≤ 0.05, **P ≤ 0.01, ***P ≤ 0.001, ****P ≤ 0.0001.

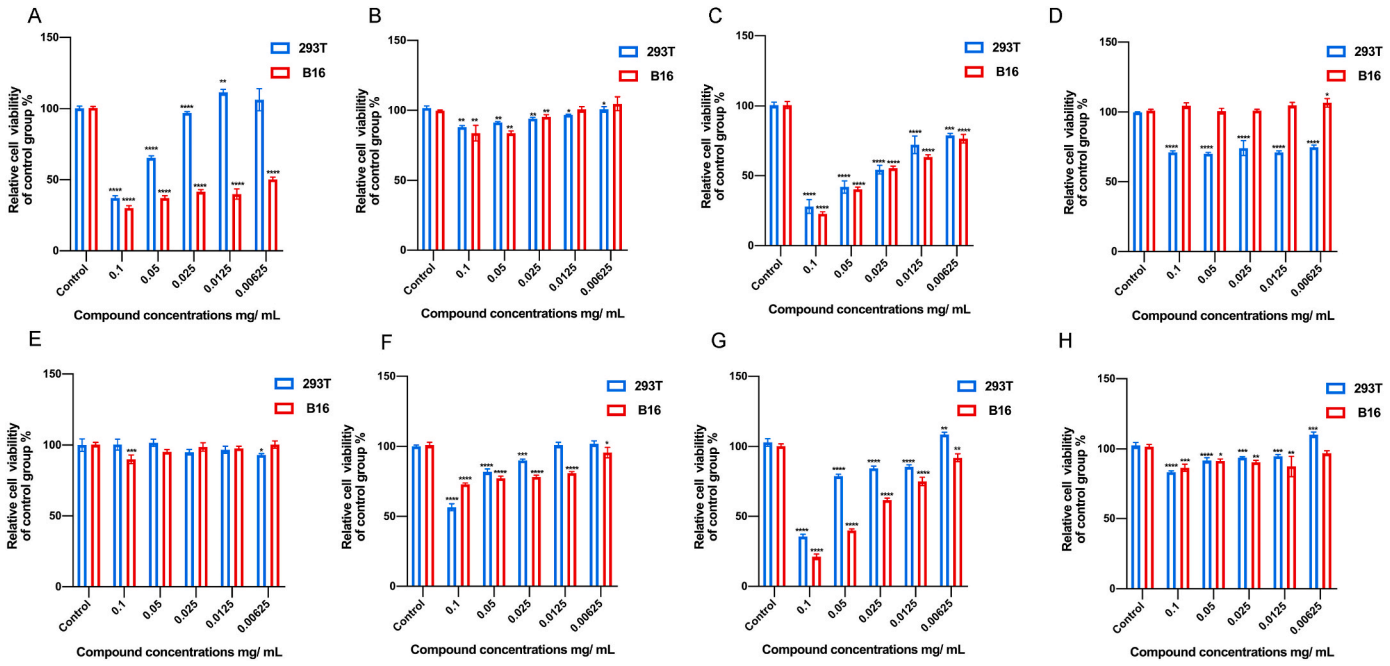

Fig. 2. Viability of 293T and B16 cells treated with different saponins, respectively, for 48 h at different concentrations. Cytotoxicity of (A) PNS; (B) PTS; (C) PDS; (D) ginsenoside Rg1; (E) ginsenoside Re; (F) ginsenoside Rb1; (G) ginsenoside Rd; (H) notoginsenoside R1. The data are expressed as a mean value ± SD of three independent experiments. Data analyses were all one-way t-tests for comparisons with the CONTROL group, *P ≤ 0.05, **P ≤ 0.01, ***P ≤ 0.001, ****P ≤ 0.0001.

water. Each measurement was conducted in triplicate. The electric potential of ethosomes was also determined as described, by injecting the diluted system into a zeta potential measurement cell.

2.9. Entrapment efficiency measurements

The entrapment efficiency of PTS in ethosome was determined after ultracentrifugation [34]. Ethosomal preparations that were kept overnight at 4 °C were spun in a TL-100 ultracentrifuge (Beckman, USA) in an ultrafiltration tube (MILIPORE) at 4 °C and 40,000 rpm for 3 h. The liquid was removed from the outer filter tube and drug quantity was determined in both the inner and outer filter tube. The entrapment efficiency was calculated as follows: [(T−C)/T] × 100%, where T is the total amount of drug, and C is the amount of drug detected only in the outer filter tube.

2.10. Determination of PTS by HPLC

PTS was analyzed by HPLC at 40 °C at the detective wavelength of 203 nm, Agilent 1100 series analytical HPLC apparatus (Palo Alto, CA, USA) was used [1]. A Zorbax ODS C18 column (250 mm × 4.6 mm i.d., 5 μm) was used at 40 °C. A binary gradient elution system consisted of water (A) and acetonitrile (B), and separation was achieved using the following gradient program: 0–30 min, 18–19% B; 30–40 min, 19–31% B; 40–60 min, 31–56% B. The flow-rate was at 1.5 mL/min and the sample injection volume was 10 μL. PTS concentration was determined from a standard curve.

2.11. UVB-induced hyperpigmentation in C57BL/6 mice

All the experimental procedures were approved by the Animal Ethics Committee, University of Macau for the welfare of experimental animals under the Animal Ethics No. UMARE-08-2020. C57BL/6 mice were purchased from the animal facility at Faculty of Health Sciences, University of Macau. All animals were maintained under constant conditions (temperature 25 ± 1 °C) and had free access to a standard diet and drinking water. UVB-induced skin hyperpigmentation was induced on the back skin of the C57BL/6 mice. The back of mice was depilated in advance and then separate areas (3 cm × 3 cm) of the back of each animal was exposed to UVB radiation (SIGMA SH-1B, Philips PLS9-01 lamp emitting 280–305 nm). The mice were randomly separated into 5 groups (n = 5 in each group). The selected skin areas were irradiated by UVB for 60 s once every two days, and the tanning was applied for two weeks. The total UVB dose was 720 mJ/cm^2 per exposure. The test compounds with different concentrations were separately mixed with carbomer gel and were given topically to the darkening back skin areas of each mouse, which was applied for two consecutive weeks every day from the next day of the last UVB irradiation. After 4 weeks, all the animals were sacrificed, and the back skin of each animal was harvested. The skin sections were then made for biopsies and histological analysis.

2.12. Hematoxylin and eosin (HE) and Fontana-Masson staining analysis

Skin biopsy specimens were fixed in 4% paraformaldehyde solution at 4 °C for 24 h. The tissue was then dehydrated and embedded in paraffin according to the standard procedures. Serial sections of 3 μm thickness were obtained. The skin histology was analyzed with HE staining [35]. We also used the Fontana-Masson that is especially for melanin stain to evaluate the melanin contents in the skin. Melanocytes and melanin were visualized using Fontana-Masson staining [36].

2.13. Determination of the melanin contents in the skin homogenate

The melanin contents in the skin homogenate were determined with a modified literature method [37]. All the skin samples were weighed and homogenized in the lysis buffer (1 N NaOH) then kept in the water bath with 80 °C for 1 h, the absorbance of extracted melanin in the skin homogenate was read at 405 nm using a multi-mode microplate reader. The final result was expressed as a percentage of the result of the control group. All the experiments were repeated for three times.

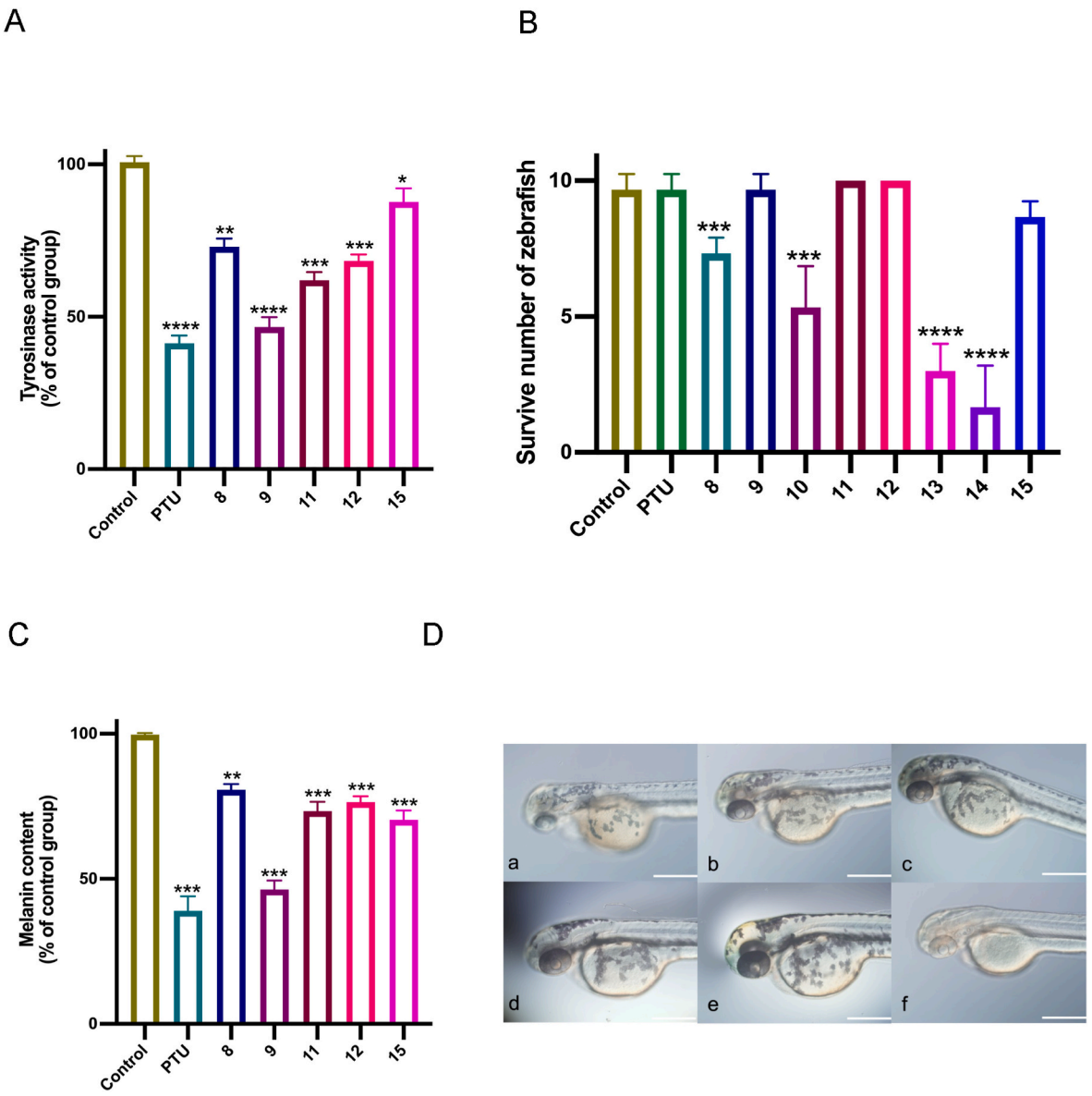

Fig. 3. Evaluation of safety and whitening activity on zebrafish embryo. (A) Effects of different saponins on zebrafish embryo tyrosinase activity. and (B) Zebrafish embryos survival results after treated with different saponins for 48h. No.8 PNS, No.9 PTS, No.10 PDS, No.11 ginsenoside Rg1, No.12 ginsenoside Re, No.13 ginsenoside Rb1, No.14 ginsenoside Rd, No.15 notoginsenoside R1. (C) Effects of different saponins on melanin synthesis of zebrafish embryo. (D) Effects of PTS on the intensity of melanin pigment were compared between the head, eye, and yolk in 72 hpf zebrafish embryos exposed to various concentrations of saponin No. 9. a.0.1mg/mL b.0.075 mg/mL c.0.050 mg/mL d.0.025 mg/mL e. control group f. PTU. Scale bar, 0.5 mm. The data are expressed as a mean value ± SD of three independent experiments. Data analyses were all one-way t-tests for comparisons with the CONTROL group, *P ≤ 0.05, **P ≤ 0.01, ***P ≤ 0.001, ****P ≤ 0.0001.

3. Results and discussion

3.1. Verification of the whitening effect of ginsenoside on B16 cells

3.1.1. Tyrosinase inhibitory activity in B16 melanoma cells

In this work, we selected five different ginsenosides and their mixtures for assessment of their whitening effects. The relationship of these five ginsenosides and mixtures is shown in Fig. 1A. The tyrosinase activity in the presence of different ginsenosides at the same concentration of 0.1mg/mL was determined and compared (Fig. 1B). PNS, PTS, PDS, ginsenoside Rg1 and ginsenoside Re showed significant tyrosinase inhibitory activity (43.7–57.2%) at 0.1 mg/mL. Meanwhile the ginsenoside Rb1, ginsenoside Rd and notoginsenoside R1 showed weak inhibition of tyrosinase activity when compared with the other groups.

3.1.2. Inhibitory effects on melanin content in B16 cells

Most of the saponins exhibited significant inhibitory effects on melanin synthesis, as shown in Fig. 1C. Particularly, the ginsenoside Rg1 and ginsenoside Re exhibited much better inhibition rates of 52.7–59.1% and 54.6–60.0%, respectively, in comparison with other saponins, which is nearly reaching the inhibition rate of PTU as the positive control.

3.2. Cytotoxicity to B16 melanoma cells and 293T cells

We examined the cytotoxicity of the five ginsenosides and their mixtures against two cell lines. The cultured cells were treated with five different concentrations of test materials for 48h, and the cell viability was assessed using MTT assays. In order to evaluate the potential cytotoxicity of saponins on normal cells, we employed 293T cell line (human renal epithelial cell line). Fig. 2 shows the effects of all the

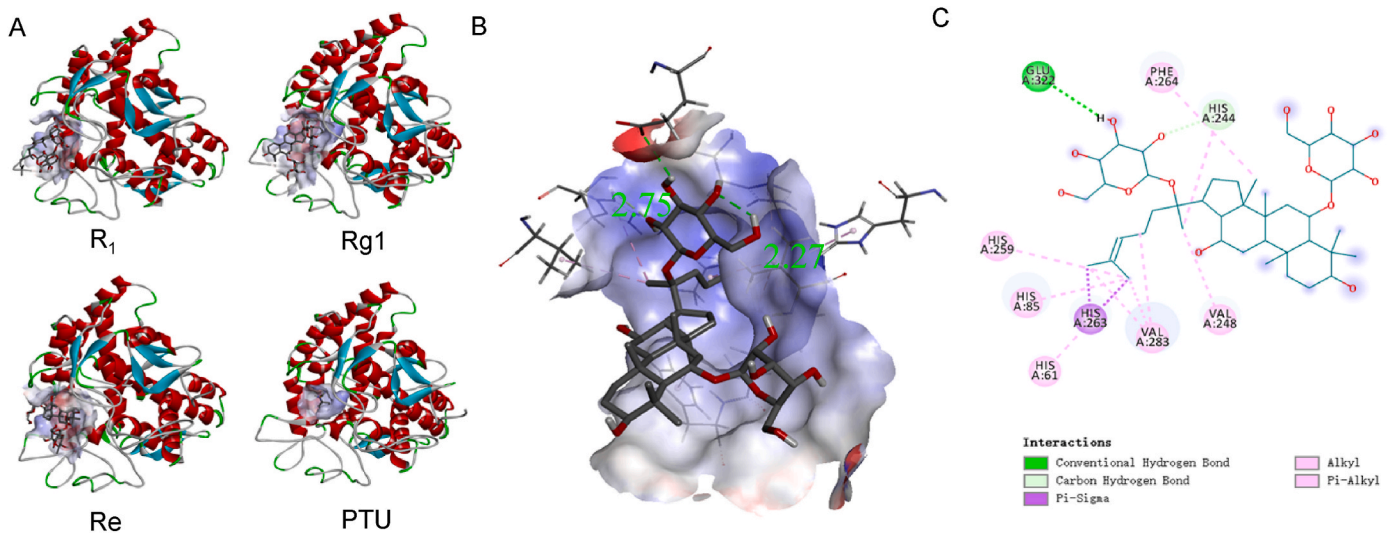

Fig. 4. Molecule docking result between tyrosinase and different saponins. (A). Binding sites and binding patterns between protein 2Y9X crystal structure of PPO3 with 3 candidate compounds and PTU. (B). 3D details of binding mode between 2Y9X and Rg1, green number showed the length of conventional hydrogen bond. (C). plat form of (B).

saponins on cell viability of 293T and B16 cells. No significant cytotoxicity was observed for PTS, ginsenoside Rg1, ginsenoside Re and notoginsenoside R1. The other saponins showed some level of toxicity to B16 cells. In particular, PNS, PDS and ginsenoside Rd showed inhibition of cellular viability on both B16 cells and 293T cells.

3.3. *Anti-melanogenic effects and toxicity of ginsenosides in zebrafish embryos*

To further address the potential of different saponins as decolorizing agents in vivo, we explored their anti-melanin production using a zebrafish embryo model and compared their decolorizing efficacy and inhibition ability of tyrosinase with PTU (the positive control agent). At the same time, the adverse effects of the tested saponins on the development of visceral organs were examined. The developmental toxicity of PTU was also examined and quantified.

After 48 h treatment, as shown in Fig. 3, at 1mg/mL, PTS significantly reduced pigmentation of zebrafish embryos in vivo without affecting the embryo development, and the treated embryos showed a high survival rate. And the saponin ginsenoside Rg1, ginsenoside Re and notoginsenoside R1 showed weak inhibition on melanin synthesis, when compared with PTS. Meanwhile, high toxicity of saponin ginsenoside Rb1 and ginsenoside Rd was observed (Fig. 3(C)), as most of the zebrafish embryos in these groups died during the treatment. The photo of different concentration PTS applied on zebrafish embryo was shown in Fig. 3(D), with no signs of cardiotoxicity observed in these zebrafish embryos, suggesting a decent safety profile of the potential decolorizing agent.

3.4. *Molecular docking*

According to the cell and zebrafish embryo results, notoginsenoside R1, ginsenoside Re and ginsenoside Rg1 and PTU were docked with 2Y9X for comparison. Among them, ginsenoside Rg1 (−6.7 kcal/mol) showed better binding affinity than PTU (−5.4 kcal/mol), but notoginsenoside R1 (−5.1 kcal/mol), ginsenoside Re (−4.9 kcal/mol), ginsenoside Rd (−5.2 kcal/mol) and ginsenoside Rb1 (−4.3 kcal/mol) were not. Binding patterns of four pairs were shown in Fig. 4(A). Binding details of 2Y9X to notoginsenoside Rg1 are shown in three-dimensional (3D) form in Fig. 4(B), which clearly indicated the spatial location of the

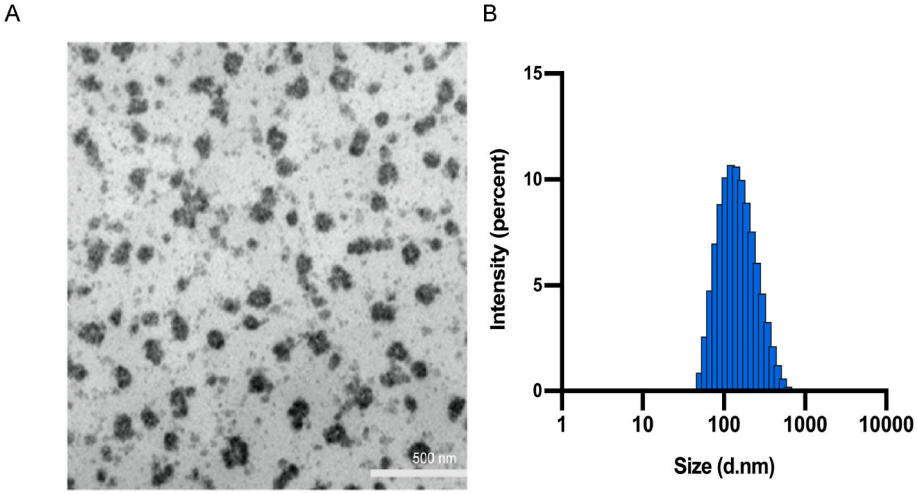

Fig. 5. Morphology and properties of PTS ethosome. (A). PTS liposome was negatively stained by phosphotungstic acid and characterized by TEM; (B). The size of PTS liposome determined by dynamic light scattering.

Table 1
The particle size, size distribution and zeta potential of PTS ethosomes stored for up to 3 months, measured via dynamic light scattering (DLS).

Time (day)	Diameter (nm)	PDI	Zeta potential (mV)
1	131.9 ± 45.6	0.198	−22.3 ± 7.08
15	137.8 ± 44.7	0.177	−23.5 ± 7.5
60	140.2 ± 35.2	0.210	−22.4 ± 7.21
90	163.3 ± 40.78	0.199	−25.2 ± 7.03

notoginsenoside R1 and the different types of bonds, as well as the lengths of the two conventional hydrogen bonds. The intermolecular hydrogen bond labelled 2.75 made the main contribution [38,39]. Details were listed in Supplement Table 1 in SI.

Considering the results of preliminary screening of different ginsenosides in the previous experiment, we found that saponin PTS, ginsenoside Rg1, ginsenoside Re and ginsenoside R1 had good whitening effects and high safety for cells and zebrafish embryos. However, ginsenoside Rb1, ginsenoside Rd and PDS were out of our consideration because of their high toxicity. Meanwhile, since the saponin ginsenoside Rg1, ginsenoside Re and ginsenoside R1 were separated from saponin PTS, we finally selected PTS as our core whitening component, which was evaluated further for dose form optimization for the whitening effects evaluation in mice.

3.5. Identification and characterization of ethosome vesicles

3.5.1. Visualization of vesicles by transmission electron microscopy

Ethosome vesicles were visualized using a transmission electron microscopy (TEM, JEOL 2100F, Japan) at the operation voltage of 200 kV. The TEM image of PTS ethosome is shown in Fig. 5(A).

3.5.2. Ethosome size and zeta potential

For the PTS ethosome prepared with 20% ethanol, the dynamic light scattering data showed a narrow particle size distribution, with an average particle size of 131 ± 45 nm (Fig. 5(B)). The zeta potential was also determined as −22.3 ± 7.08 mV. The stability of size and zeta potential were also determined after storage for three months. As shown in Table 1 and Fig. S1, we successful attained a PTS ethosome with an entrapment efficiency of as high as 93% and the size and zeta potential could be maintained stable for three months.

3.6. Whitening effects on UVB tanning C57BL/6 mouse model

3.6.1. UVB induced pigmentation on C57BL/6 mouse model

The UVB induced pigmentation in mice was established as shown in Fig. 6(A). When compared with the normal control group, the back of mice irradiated with UVB turned to much darker without obvious swollen or inflammatory signs. All the mice were in good condition until the experiment finished.

3.6.2. PTS ethosomes reduced the melanin content in the back skin of UVB tanning C57BL/6 mice

Microscopic and histopathological analysis of back skin of mice showed no significant burns or injuries in any areas of the dorsal skin of mice (Fig. 6). We further determined the melanin contents of the back skin homogenate of each group. As shown in Fig. 6(B). When compared

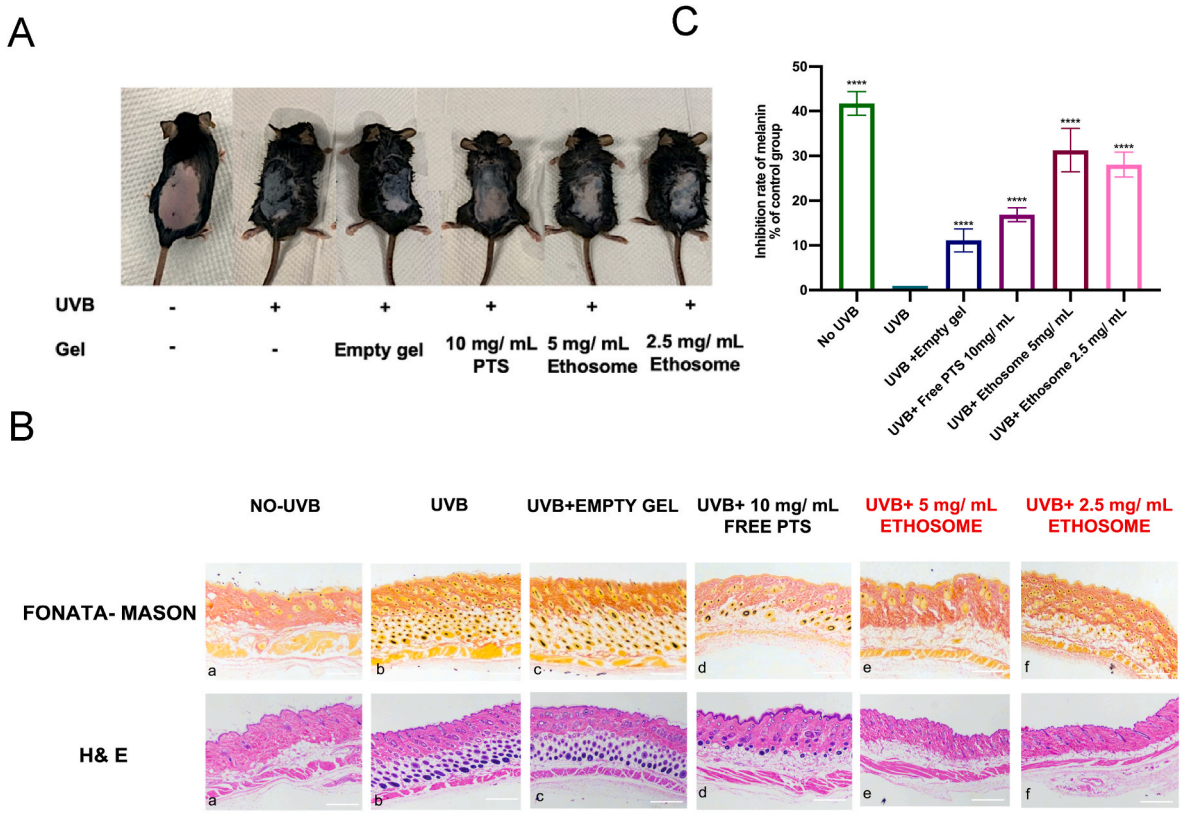

Fig. 6. Figure of UVB induced tanning model and treatment result. (A). Photo of rat back of different group after experiment; (B). Relative melanin inhibition rate of in the homogenates of pigmented skins. The results were shown by the difference between the melanin content of different groups and the UVB only group. The data are expressed as a mean value + SD of five independent experiments; (C) Fontana-mason (first line) and Hematoxylin and eosin (HE) staining (second line) results of effects of the different group (two weeks of treatment) on UVB tanning in C57BL/6 mouse skins. (a) Control group without UVB irradiation. (b) UVB irradiation only (c) UVB irradiation and applied with empty gel. (d) UVB irradiation and applied with 10mg/mL free PTS. (e) UVB irradiation and applied with 5 mg/mL PTS ethosome. (f) UVB irradiation and applied with 5 mg/mL PTS ethosome. The data are expressed as a mean value ± SD of three independent experiments. Data analyses were all one-way t-tests for comparisons with the CONTROL group, *P ≤ 0.05, **P ≤ 0.01, ***P ≤ 0.001, ****P ≤ 0.0001.

with the control group, both free PTS and PTS ethosome group reduced the content of melanin in the back skin of mice, and the ethosome group showed the much lower concentration of melanin (5 mg/mL) than that (10 mg/mL) of free PTS treated group. The results fully validated the improvement of skin delivery efficiency of ethosome dosage forms. Meanwhile the results of hematoxylin and eosin (HE) staining and Fontana-Masson (Fig. 6(C)) showed us more visually that melanin in the dorsal skin of mice increased after UVB radiation, but decreased significantly after treatment with free PTS and ethosome containing different PTS levels, indicating the excellent skin whitening effect of PTS.

4. Conclusion

A safety skin lightning agent has been strived for many researchers. To inhibit the synthesis of melanin, the key point is to inhibit the activity of tyrosinase which is a copper-containing enzyme that plays a crucial role in the production of melanin [40]. In this work, we first screened for safe and efficient depigmentation agents from different ginsenosides isolated from Panax ginseng using B16 melanoma cells and zebrafish embryo models [41–44]. Further molecular docking work also verified the binding affinity of the saponins in PTS with tyrosinase. Compared to tyrosinase with a fixed crystal structure in molecular docking, proteins in solution may have various conformations and produce different binding affinity with small molecules, which results in poorer Rg1 activity in experiments compared to PTU, but exhibits a better affinity in molecular docking.

As a result, we finally found that ginsenoside PTS, showed potential skin whitening ability and no significant side effects on cells and zebrafish embryos. Regarding the effect of cytotoxicity on tyrosinase activity, according to the literature, cell viability does affect tyrosinase activity, which in turn reduces the amount of melanin in the cells [45]. This could also reveal that PNS, while possessing a higher toxicity, also has a better melanin inhibiting ability and was therefore excluded from our selection. Therefore, we chose saponins with good safety and whitening effect, which have been excluded from interfering with tyrosinase activity by cellular viability.

Then in order to increase the skin penetration of the drug and to increase the transdermal absorption of the whitening product, we developed the ethosome system for the skin delivery of PTS [46,47]. After several experiments, we obtained a relatively stable and optimized formulation: soy lecithin 9%, cholesterol 4%, ethanol 20%, PTS as described, water 100% w/w, size 131 $\pm$ 4 nm, zeta potential -22.3 mV, and can be stored stably at -4 °C for 3 months. We tested the whitening effect of PTS ethosome using a UVB tanning C57BL/6 mouse model in order to better illustrate the effective delivery of PTS ethosome. Additionally, the PTS ethosome group showed melanin inhibition after 4 weeks of therapy. Additionally, even at lesser concentrations, the PTS ethosome group's whitening impact outperformed the free PTS group's. This research fully supports the great improvement in skin delivery effectiveness of the ethosome dosage form and also provides fresh insights into the transdermal distribution of water-soluble natural products. Previously, many works mainly applied ginsenoside monomer or monomer derivatives as the main whitening ingredients for development, and for the first time, we used PTS, a mixture of saponins isolated from P. notoginseng, to maximize the therapeutic effect as well as the great improvement of safety [48,49]. Considering that the content of saponins in P. notoginseng is high and the cost of P. notoginseng is lower compared with that of P. ginseng, the cost can be better controlled when it is developed into a whitening product. This work provides more references for the development of ginsenosides as a bleaching agent for cosmetic bleaching agents.

Declaration of competing interest

The authors declare no conflicts of interest.

Acknowledgements

This work was supported by the Science and Technology Development Fund of Macau SAR (FDCT 0007/2021/ITP and 0065/2021/A2).

Appendix A. Supplementary data

Supplementary data to this article can be found online at https://doi.org/10.1016/j.jgr.2023.12.005.

References

[1] Wan J, Yang F, Li S, Wang Y, Cui X. Chemical characteristics for different parts of Panax notoginseng using pressurized liquid extraction and HPLC-ELSD. J Pharmaceut Biomed Anal 2006;41(5):1596–601.
[2] Baeg I-H, So S-H. The world ginseng market and the ginseng (Korea). J Ginseng Res 2013;37(1):1.
[3] Hao Y-J, An X-L, Sun H-D, Piao X-C, Gao R, Lian M-L. Ginsenoside synthesis of adventitious roots in Panax ginseng is promoted by fungal suspension homogenate of Alternaria panax and regulated by several signaling molecules. Ind Crop Prod 2020;150:112414.
[4] Wan JB, Li Sp, Chen JM, Wang YT. Chemical characteristics of three medicinal plants of the Panax genus determined by HPLC-ELSD. J Separ Sci 2007;30(6):825–32.
[5] Ng T. Pharmacological activity of sanchi ginseng (Panax notoginseng). J Pharm Pharmacol 2006;58(8):1007–19.
[6] Chu LL, Montecillo JAV, Bae H. Recent advances in the metabolic engineering of yeasts for ginsenoside biosynthesis. Front Bioeng Biotechnol 2020;8:139.
[7] Cen Y, Fa-Xiang X, Huang X-J, Shao-Ping L, Zhang Q-W. A novel 12, 23-epoxy dammarane saponin from PanaPanax notoginseng. Chin J Nat Med 2015;13(4):303–6.
[8] Xu F-X, Yuan C, Wan J-B, Yan R, Hu H, Li S-P, Zhang Q-W. A novel strategy for rapid quantification of 20 (S)-protopanaxatriol and 20 (S)-protopanaxadiol saponins in Panax notoginseng P. ginseng and P. quinquefolium. Nat Prod Res 2015;29(1):46–52.
[9] Wan J-B, Li P, Yang R-L, Zhang Q-W, Wang Y-T. Separation and purification of 5 saponins from Panax notoginseng by preparative high-performance liquid chromatography. J Liq Chromatogr Relat Technol 2013;36(3):406–17.
[10] Li S, Qiao C, Chen Y, Zhao J, Cui X, Zhang Q, Liu X, Hu D. A novel strategy with standardized reference extract qualification and single compound quantitative evaluation for quality control of Panax notoginseng used as a functional food. J Chromatogr A 2013;1313:302–7.
[11] Chang T-S. An updated review of tyrosinase inhibitors. Int J Mol Sci 2009;10(6):2440–75.
[12] Costin G-E, Hearing VJ. Human skin pigmentation: melanocytes modulate skin color in response to stress. Faseb J 2007;21(4):976–94.
[13] Yu X, Du L, Li Y, Fu G, Jin Y. Improved anti-melanoma effect of a transdermal mitoxantrone ethosome gel. Biomed Pharmacother 2015;73:6–11.
[14] Touitou E, Dayan N, Bergelson L, Godin B, Eliaz M. Ethosomes—novel vesicular carriers for enhanced delivery: characterization and skin penetration properties. J Contr Release 2000;65(3):403–18.
[15] Harris RA, Burnett R, McQuilkin S, McClard A, Simon FR. Effects of ethanol on membrane order: fluorescence studies a. Ann N Y Acad Sci 1987;492(1):125–35.
[16] Lynn Lamoreux M, Kelsh RN, Wakamatsu Y, Ozato K. Pigment pattern formation in the medaka embryo. Pigm Cell Res 2005;18(2):64–73.
[17] Love DR, Pichler FB, Dodd A, Copp BR, Greenwood DR. Technology for high-throughput screens: the present and future using zebrafish. Curr Opin Biotechnol 2004;15(6):564–71.
[18] Peterson RT, Link BA, Dowling JE, Schreiber SL. Small molecule developmental screens reveal the logic and timing of vertebrate development. Proc Natl Acad Sci USA 2000;97(24):12965–9.
[19] Zon LI, Peterson RT. In vivo drug discovery in the zebrafish. Nat Rev Drug Discov 2005;4(1):35–44.
[20] Choi TY, Kim JH, Ko DH, Kim CH, Hwang JS, Ahn S, Kim SY, Kim CD, Lee JH, Yoon TJ. Zebrafish as a new model for phenotype-based screening of melanogenic regulatory compounds. Pigm Cell Res 2007;20(2):120–7.
[21] Yamada T, Hasegawa S, Inoue Y, Date Y, Yamamoto N, Mizutani H, Nakata S, Matsunaga K, Akamatsu H. Wnt/β-catenin and kit signaling sequentially regulate melanocyte stem cell differentiation in UVB-induced epidermal pigmentation. J Invest Dermatol 2013;133(12):2753–62.
[22] Rosdahl IK. Local and systemic effects on the epidermal melanocyte population in UV-irradiated mouse skin. J Invest Dermatol 1979;73(4):306–9.
[23] Wang Y-T, Zhang Q-W, Wan J-B. Separation and purification of protopanaxatriol and protopanaxadiol type saponins from Panax notoginseng with macroporous resins (Refereed). 2008.
[24] Ando H, Itoh A, Mishima Y, Ichihashi M. Correlation between the number of melanosomes, tyrosinase mRNA levels, and tyrosinase activity in cultured murine melanoma cells in response to various melanogenesis regulatory agents. J Cell Physiol 1995;163(3):608–14.
[25] Ding HY, Chang TS, Shen HC, Tai SSK. Murine tyrosinase inhibitors from Cynanchum bungei and evaluation of in vitro and in vivo depigmenting activity. Exp Dermatol 2011;20(9):720–4.

[26] Jeong YT, Jeong SC, Hwang JS, Kim JH. Modulation effects of sweroside isolated from the Lonicera japonica on melanin synthesis. Chem Biol Interact 2015;238:33–9.
[27] Hu W-J, Yan L, Park D, Jeong HO, Chung HY, Yang J-M, Ye ZM, Qian G-Y. Kinetic, structural and molecular docking studies on the inhibition of tyrosinase induced by arabinose. Int J Biol Macromol 2012;50(3):694–700.
[28] Wang Y, Zhang G, Yan J, Gong D. Inhibitory effect of morin on tyrosinase: insights from spectroscopic and molecular docking studies. Food Chem 2014;163:226–33.
[29] Ashraf Z, Rafiq M, Seo S-Y, Babar MM. Synthesis, kinetic mechanism and docking studies of vanillin derivatives as inhibitors of mushroom tyrosinase. Bioorg Med Chem 2015;23(17):5870–80.
[30] Biovia DS. Discovery studio modeling environment. 2017. Release.
[31] Trott O, Olson AJ. AutoDock Vina: improving the speed and accuracy of docking with a new scoring function, efficient optimization, and multithreading. J Comput Chem 2010;31(2):455–61.
[32] Kim S, Chen J, Cheng T, Gindulyte A, He J, He S, Li Q, Shoemaker BA, Thiessen PA, Yu B. PubChem 2019 update: improved access to chemical data. Nucleic Acids Res 2019;47(D1):D1102–9.
[33] Seo S-Y, Sharma VK, Sharma N. Mushroom tyrosinase: recent prospects. J Agric Food Chem 2003;51(10):2837–53.
[34] Heeremans J, Gerrttsen H, Meusen S, Mijnheer F, Gangaram Panday R, Prevost R, Kluft C, Crommelin D. The preparation of tissue-type plasminogen activator (t-PA) containing liposomes: entrapment efficiency and ultracentrifugation damage. J Drug Target 1995;3(4):301–10.
[35] Katano H, Sato Y, Tsutsui Y, Sata T, Maeda A, Nozawa N, Inoue N, Nomura Y, Kurata T. Pathogenesis of cytomegalovirus-associated labyrinthitis in a Guinea pig model. Microb Infect 2007;9(2):183–91.
[36] Yoon T-J, Lei TC, Yamaguchi Y, Batzer J, Wolber R, Hearing VJ. Reconstituted 3-dimensional human skin of various ethnic origins as an in vitro model for studies of pigmentation. Anal Biochem 2003;318(2):260–9.
[37] Peng L-H, Liu S, Xu S-Y, Chen L, Shan Y-H, Wei W, Liang W-Q, Gao J-Q. Inhibitory effects of salidroside and paeonol on tyrosinase activity and melanin synthesis in mouse B16F10 melanoma cells and ultraviolet B-induced pigmentation in Guinea pig skin. Phytomedicine 2013;20(12):1082–7.
[38] Ferreira de Freitas R, Schapira M. A systematic analysis of atomic protein-ligand interactions in the PDB. Medchemcomm 2017;8(10):1970–81.
[39] Schiebel J, Gaspari R, Wulsdorf T, Ngo K, Sohn C, Schrader TE, Cavalli A, Ostermann A, Heine A, Klebe G. Intriguing role of water in protein-ligand binding studied by neutron crystallography on trypsin complexes. Nat Commun 2018;9(1):3559.
[40] Jimbow K, Obata H, Pathak MA, Fitzpatrick TB. Mechanism of depigmentation by hydroquinone. J Invest Dermatol 1974;62(4):436–49.
[41] Wu X, Guy RH. Applications of nanoparticles in topical drug delivery and in cosmetics. J Drug Deliv Sci Technol 2009;19(6):371–84.
[42] Kelsh RN, Brand M, Jiang YJ, Heisenberg CP, Lin S, Haffter P, Odenthal J, Mullins MC, van Eeden FJ, Furutani-Seiki M, et al. Zebrafish pigmentation mutations and the processes of neural crest development. Development 1996;123:369–89.
[43] Hirata M, Nakamura K, Kondo S. Pigment cell distributions in different tissues of the zebrafish, with special reference to the striped pigment pattern. Dev Dynam 2005;234(2):293–300.
[44] Pichler FB, Laurenson S, Williams LC, Dodd A, Copp BR, Love DR. Chemical discovery and global gene expression analysis in zebrafish. Nat Biotechnol 2003;21(8):879–83.
[45] Barros MR, Menezes TM, da Silva LP, Pires DS, Princival JL, Seabra G, Neves JL. Furan inhibitory activity against tyrosinase and impact on B16F10 cell toxicity. Int J Biol Macromol 2019;136:1034–41.
[46] Jaiswal PK, Kesharwani S, Kesharwani R, Patel DK. Ethosome: a new technology used as topical & transdermal delivery system. J Drug Deliv Therapeut 2016;6(3):7–17.
[47] Dave V, Kumar D, Lewis S, Paliwal S. Ethosome for enhanced transdermal drug delivery of aceclofenac. Int J Drug Deliv 2010;2(1).
[48] Jin Y, Kim JH, Hong H-D, Kwon J, Lee EJ, Jang M, Lee S-Y, Han A-R, Nam TG, Hong SK. Ginsenosides Rg5 and Rk1, the skin-whitening agents in black ginseng. J Funct Foods 2018;45:67–74.
[49] Kim JH, Baek EJ, Lee EJ, Yeom MH, Park JS, Lee KW, Kang NJ. Ginsenoside F1 attenuates hyperpigmentation in B16F10 melanoma cells by inducing dendrite retraction and activating Rho signalling. Exp Dermatol 2015;24(2):150–2.